

# Analytic Score Optimization for Multi Dimension Video Quality Assessment

Boda Lin<sup>\*</sup> <sup>1</sup> Yongjie Zhu<sup>†</sup> <sup>1</sup> Wenyu Qin <sup>1</sup> Meng Wang <sup>1</sup> Pengfei Wan <sup>1</sup>

## Abstract

Video Quality Assessment (VQA) is evolving beyond single-number mean opinion score toward richer, multi-faceted evaluations of video content. In this paper, we present a large-scale multi-dimensional VQA dataset UltraVQA that encompasses diverse User-Generated Content (UGC) annotated across five key quality dimensions: Motion Quality, Motion Amplitude, Aesthetic Quality, Content Quality, and Clarity Quality. Each video in our dataset is scored by over 3 human raters on these dimensions, with fine-grained sub-attribute labels, and accompanied by an explanatory rationale generated by GPT based on the collective human judgments. To better leverage these rich annotations and improve discrete quality score assessment, we introduce Analytic Score Optimization (ASO), a theoretically grounded post-training objective derived for multi-dimensional VQA. By reframing quality assessment as a regularized decision-making process, we obtain a closed-form solution that naturally captures the ordinal nature of human ratings, ensuring alignment with human ranking preferences. In experiments, our method outperforms most baselines including closed-source APIs and open-source models, while also reducing mean absolute error (MAE) in quality prediction. Our work highlights the importance of multi-dimensional, interpretable annotations and reinforcement-based alignment in advancing video quality assessment.

## 1. Introduction

Assessing the perceptual quality of videos remains a long-standing challenge in computer vision and multimedia processing. Traditional VQA methods often reduce perceptual

<sup>\*</sup>This work was conducted during the author's internship at Kling Team, Kuaishou Technology. <sup>†</sup>Project learner.

<sup>1</sup>Kling Team, Kuaishou Technology, Beijing, China. Correspondence to: Yongjie Zhu <zhuyongjie@kuaishou.com>.

Preprint. February 20, 2026.

quality to a single scalar, most commonly the Mean Opinion Score (MOS), whether they are hand-crafted no-reference metrics or early learning-based models. While convenient for benchmarking and optimization, a single score is inherently limited: it obscures why a video is perceived as good or bad, and cannot disentangle the diverse factors that jointly shape viewers' quality of experience (Pu et al., 2025). As user-generated content (UGC) becomes increasingly diverse in style, capture conditions, and post-processing, there is a growing demand for multi-dimensional VQA that evaluates quality along multiple, more interpretable axes (Duan et al., 2025; He et al., 2025).

Recent work has begun to move in this direction by decomposing video quality into multiple aspects such as spatial quality, temporal consistency, and aesthetics (Zhang et al., 2023; Duan et al., 2025; Wu et al., 2023a; He et al., 2025; Pu et al., 2025). For example, MD-VQA (Zhang et al., 2023) studies semantic, distortion, and motion factors for UGC livestream videos, while MVQA (Pu et al., 2025) emphasizes multi-factor quality understanding with richer annotations. More recently, vision-language models (VLMs) have been applied to VQA, bringing stronger high-level reasoning and the ability to produce textual explanations beyond pixel-level cues (Pu et al., 2025; He et al., 2025). Despite this progress, existing VLM-based VQA systems still face two practical limitations. First, models often yield coarse overall judgments and are insufficiently sensitive to nuanced quality factors (e.g., subtle motion artifacts or aesthetic trade-offs), especially under distribution shifts. Second, in the absence of carefully curated training data with consistent multi-dimensional labels and rationale supervision, even strong VLMs can exhibit weak correlation with human ratings on standard benchmarks (citation to be added).

To address these challenges, we introduce a large-scale VQA dataset, UltraVQA, designed for both comprehensiveness and interpretability. UltraVQA characterizes video quality using five core dimensions: (1) **Motion Quality**, capturing temporal smoothness and stability; (2) **Motion Amplitude**, measuring the degree and extent of motion; (3) **Aesthetic Quality**, reflecting perceived visual appeal such as composition and lighting; (4) **Content Quality**, assessing semantic relevance and meaningfulness; and (5) **Clarity Quality**, covering sharpness, resolution, noise, and compression artifacts.

Each dimension further includes fine-grained sub-attributes, enabling models to learn structured quality judgments rather than conflating heterogeneous factors into a single score.

Beyond scores and sub-attributes, UltraVQA also provides explanatory rationales for improved transparency. We employ 40 specially trained annotators, and each video clip is scored by at least three annotators across all five dimensions, together with detailed attribution tags. We further use GPT-4.1 to synthesize concise rationale paragraphs that explain the assigned scores based on the human-provided ratings and tags. This rationale supervision is intended to encourage models to not only predict scores but also justify their evaluations.

In multi-dimensional VQA, the supervision signal is fundamentally ordinal and discrete: each dimension is rated on a small set of levels (e.g., 1.0–5.0 with 0.5 steps used in our UltraVQA), and the evaluation emphasizes rank or linear agreement rather than exact regression to a continuous MOS. However, most post-training pipelines treat scoring either as (i) free-form generation with sparse correctness rewards, or (ii) continuous regression, both of which ignore the finite, ordered label space and often yield poorly calibrated score distributions. This mismatch becomes particularly problematic for motion-centric dimensions, where the perceived difference between adjacent levels can be subtle and policy-gradient updates are high-variance. Motivated by this, we introduce Analytic Score Optimization (ASO): instead of relying on stochastic policy gradients, we formulate discrete scoring as a KL-regularized one-step bandit and derive a closed-form optimal score policy over discrete levels. ASO turns discrete score alignment into a stable, sample-efficient soft-target learning objective, which complements standard RL alignment and directly exploits the structure of ordinal score spaces.

We validate our approach on UltraVQA as well as multiple public benchmarks. Experiments show that VLM trained with ASO achieves improvements over strong baselines, and that training with rationale supervision yields more faithful explanations and improved performance.

In summary, our contributions are:

- **Dataset:** We construct UltraVQA, a large-scale multi-dimensional VQA dataset with five quality dimensions and fine-grained sub-attributes. Each clip is annotated by multiple trained annotators and accompanied by rationale explanations synthesized from human annotations.
- **Method:** We introduce Analytic Score Optimization (ASO), an RL-inspired analytic optimization objective tailored to discrete quality scoring with a finite label space.

- **Results:** We demonstrate consistent gains on UltraVQA and public benchmarks, and show that rationale supervision improves interpretability and zero-shot generalization.

## 2. Related Work

### 2.1. VQA Datasets

Over the past decade, numerous VQA datasets have been established to advance video quality assessment. Early datasets (Ghadiyaram et al., 2017; Nuitinen et al., 2016; Sinno & Bovik, 2018; Wang et al., 2016; 2017; 2021; Yu et al., 2021) often used limited source videos with synthetic distortions like compression and transmission errors. Later “in-the-wild” UGC datasets such as KoNViD-1k (Hosu et al., 2017), YouTube-UGC (Wang et al., 2019), and LSVQ (Ying et al., 2021) collected real-world videos with diverse authentic distortions. These benchmarks typically provide a single MOS per video as the ground-truth quality. While valuable, single-score datasets have inherent limitations that they do not reveal which aspect of quality influenced the rating, and models trained on them can struggle to generalize across content types (Duan et al., 2025; Zhang et al., 2023; Liu et al., 2022; Chen et al., 2021; Wu et al., 2023b). Recognizing the multi-faceted nature of video quality, researchers have begun exploring multi-dimensional VQA. MD-VQA (Zhang et al., 2023) introduced a concept of multi-dimensional quality for UGC live videos, focusing on three dimensions (semantic quality, distortion, motion) and even proposed an interpretable model that fuses features corresponding to these factors. Their results showed better performance than one-dimensional approaches, confirming the benefit of multi-dim labels. Our work extends this line by covering a broader set of quality dimensions, including subjective aesthetics and content coherence, and by scaling up to a much larger dataset. Most closely related to our dataset is the very recent MVQA-68K benchmark (Pu et al., 2025), which independently also emphasizes multi-dimensional annotation (seven dimensions including aesthetics, motion, etc.) and provides chain-of-thought reasoning for interpretability. Our dataset differs in the specific taxonomy of quality dimensions (we define five major categories tailored to UGC, whereas MVQA-68K uses seven slightly different ones) and in the scale of human annotation per video (30+ ratings each, enabling robust consensus).

### 2.2. VQA Methods

Traditional VQA methods can be classified into full-reference (FR), reduced-reference, and no-reference (NR) methods. FR methods (e.g., PSNR, SSIM, VMAF) assume access to an undistorted reference video and compute differences, which is impractical for UGC. NR methods rely on learning-based features or hand-crafted features to pre-

dict quality directly from the distorted video. Before the deep learning era, NR-VQA models used features targeting distortions like blockiness or blur. More recent deep learning models (e.g., VSFA, TLVQM, PVQ, etc.) learn to regress MOS from deep CNN or CNN with LSTM features of video frames. However, these approaches usually still output a single score per video, lacking interpretability. The NR-VQA model in MD-VQA (Zhang et al., 2023), for instance, improved performance by explicitly modeling multiple factors (using separate CNNs for semantic, distortion, motion features and fusing them), but its output remained an overall MOS, and the interpretability came from the model architecture rather than human-readable explanations.

### 2.3. VLM and Post-training

Due to their strong generalization and instruction-following capability, Vision-Language Models (VLMs) are increasingly adopted as versatile backbones for VQA task. Representative frameworks (e.g., LLaVA (Liu et al., 2023), BLIP-2 (Li et al., 2023), Flamingo (Alayrac et al., 2022), Kosmos-2 (Peng et al., 2023)) demonstrate effective recipes for coupling vision encoders with LLMs to enable multimodal reasoning and structured generation. Recent open-source families such as Qwen-VL (Yang et al., 2025; Bai et al., 2025; Wang et al., 2024), MiniCPM-V (Yu et al., 2025), and InternVL (Zhu et al., 2025; Chen et al., 2025) further strengthen accessibility and practical deployment.

Compared to conventional NR-VQA regressors, VLM-based scorers can incorporate higher-level semantic cues (e.g., content coherence) and provide more interpretable outputs. Nevertheless, reliable quality scoring requires post-training: models must learn (i) strict output formats, (ii) calibrated discrete scoring behaviors, and (iii) alignment with human rating criteria across diverse content domains.

Direct Preference Optimization (DPO) (Rafailov et al., 2023) is a widely adopted method. Subsequent works propose reference-free or simplified variants, such as ORPO (Hong et al., 2024) and SimPO (Meng et al., 2024), as well as objectives that learn from weaker binary signals, e.g., KTO (Ethayarajh et al., 2024). More recently, Implicit Preference Optimization (IPO) views LMs as implicit preference classifiers, further reducing reliance on explicit reward modeling (Garg et al., 2025). These approaches are particularly attractive for VQA settings where supervision can be naturally expressed as pairwise preferences (e.g., which video looks better) or ordinal levels.

RLHF typically optimizes a learned reward model with online policy updates, where PPO is a standard choice due to its stability (Schulman et al., 2017). However, online RL can be memory- and compute-intensive, motivating more efficient alternatives such as GRPO (Shao et al., 2024) in large-scale practice.

## 3. Dataset

### 3.1. Data Collection

UltraVQA contains approximately 40,000 video clips curated from a mixture of in-the-wild UGC platforms and professional content sources, covering diverse genres such as vlogs, sports, gaming, education, interviews, and cinematic edits.

We ensured diversity in the footage: videos include both camera-captured authentic content and some AI-generated or edited content, to reflect modern video sources. We also intentionally included a subset of professionally produced or artistically edited high-aesthetic clips to counterbalance the fact that many widely used VQA datasets are dominated by imperfect/distorted UGC and contain relatively few truly high-quality samples (Hosu et al., 2017; Ying et al., 2021; Götz-Hahn et al., 2021; Sinno & Bovik, 2018).

### 3.2. Quality Dimensions and Sub-attributes

We annotate five complementary quality dimensions: Motion Quality (temporal smoothness and stability), Motion Amplitude (degree/extents of motion), Aesthetic Quality (composition, color, lighting, and overall visual appeal), Content Quality (semantic coherence, informativeness, and subject completeness), and Clarity Quality (sharpness, resolution, noise, and compression artifacts). For each dimension, raters additionally select fine-grained sub-attribute tags from a curated checklist (e.g., camera shake, motion blur, over-compression, poor lighting). These tags enable more structured error analysis and serve as grounded evidence for rationale synthesis. The details of tags are shown in Appendix B.

### 3.3. Data Statistics

The statistical details of our UltraVQA are shown in the Figure 1. Considering the current processing power of VLM and the limitations of GPU memory, we divide most of the videos into segments of less than 30 seconds, and retained a small number of videos longer than 30 seconds. To ensure the UltraVQA covers as many visual quality levels as possible, we select videos ranging from 480p to 4K resolution. Notably, videos at 4K and higher resolutions comprise 16.5% of our UltraVQA. We maintain the original FPS for all videos to the greatest extent possible, covering a variety of common video standards, including Cinema, PAL, NTSC, etc. In addition, the average number of annotation tokens is 94.75 and the average number of annotation words for each video is 76.95. Finally, we analyzed the thematic range of the videos, as shown in the Figure 1, which includes 16 major categories.

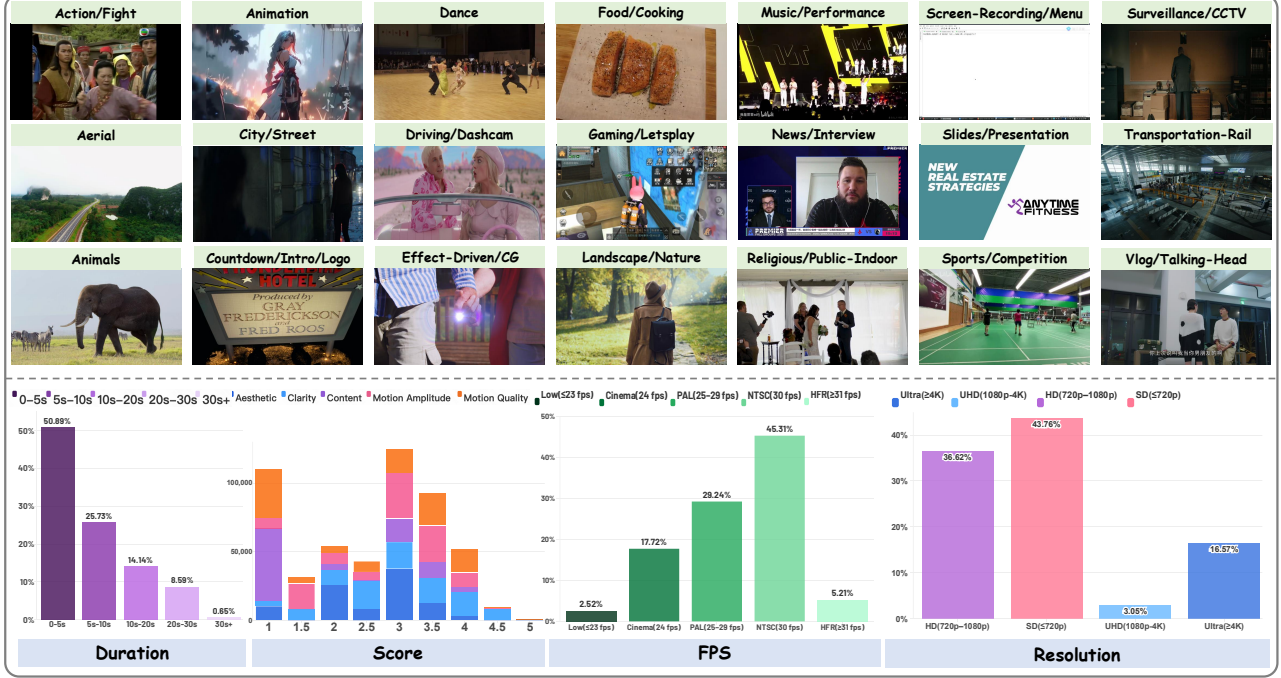


Figure 1. Cases for each category and distribution of statistics of our UltraVQA.

### 3.4. Data Annotation

The dataset annotation process is shown in the Figure 2.

To capture the multifaceted nature of User-Generated Content (UGC), we established a hierarchical annotation taxonomy covering both high-level quality dimensions and fine-grained attribution tags.

**Quality Dimensions and Fine-grained Attributes.** We define five complementary quality dimensions: Motion Quality, Motion Amplitude, Aesthetic Quality, Content Quality, and Clarity Quality. Unlike previous datasets that rely solely on holistic scoring, we require annotators to provide grounded evidence for their ratings. For each dimension, annotators must select applicable sub-attributes from a curated checklist of failure modes and highlights. For instance, Clarity Quality includes tags such as Blur, Noise/Grain, and Compression Artifacts, while Aesthetic Quality covers attributes like Composition, Lighting, and Color Grading. These categorical tags serve a dual purpose: they enable structured error analysis and act as “anchor points” for generating hallucinogen-free textual rationales.

**Robust Annotation Protocol.** We engaged a pool of 40 trained professional annotators to ensure consistency. The annotation process follows a rigorous redundancy protocol where each video clip is independently evaluated by at least three annotators. Raters assess each dimension on a 5-point Likert scale (1.0 to 5.0, with 0.5 intervals), accompanied by the selection of relevant tags. To mitigate subjective bias in-

herent in UGC assessment, we implement a post-processing filtering step: annotations with excessive variance or inconsistency are flagged and re-evaluated. The final ground-truth score for each dimension is derived through statistical aggregation (typically the mean) of valid ratings, ensuring a robust distribution aligned with human perception.

**Evidence-Grounded Rationale Synthesis.** Beyond numerical scores, UltraVQA provides interpretable textual supervision. Directly collecting free-form comments from crowd-workers often yields noisy or sparse text. Instead, we propose an evidence-grounded synthesis pipeline. We aggregate the human-selected sub-attribute tags and raw comments to form a structured “evidence set.” We then prompt GPT-4.1 to synthesize a concise, coherent rationale conditioned strictly on: (i) the visual content, (ii) the aggregated ground-truth score, and (iii) the collective human evidence. This approach distills the consensus of multiple human raters into high-quality natural language, ensuring that the generated rationales are not model hallucinations but are faithfully grounded in human judgment.

## 4. Method

Consistent with common post-training practice, we first perform supervised fine-tuning (SFT) on a vision-language model (VLM) to equip it with reliable formatted outputs and a basic capability for video quality scoring. We then apply GRPO on top of the SFT checkpoint to further improve

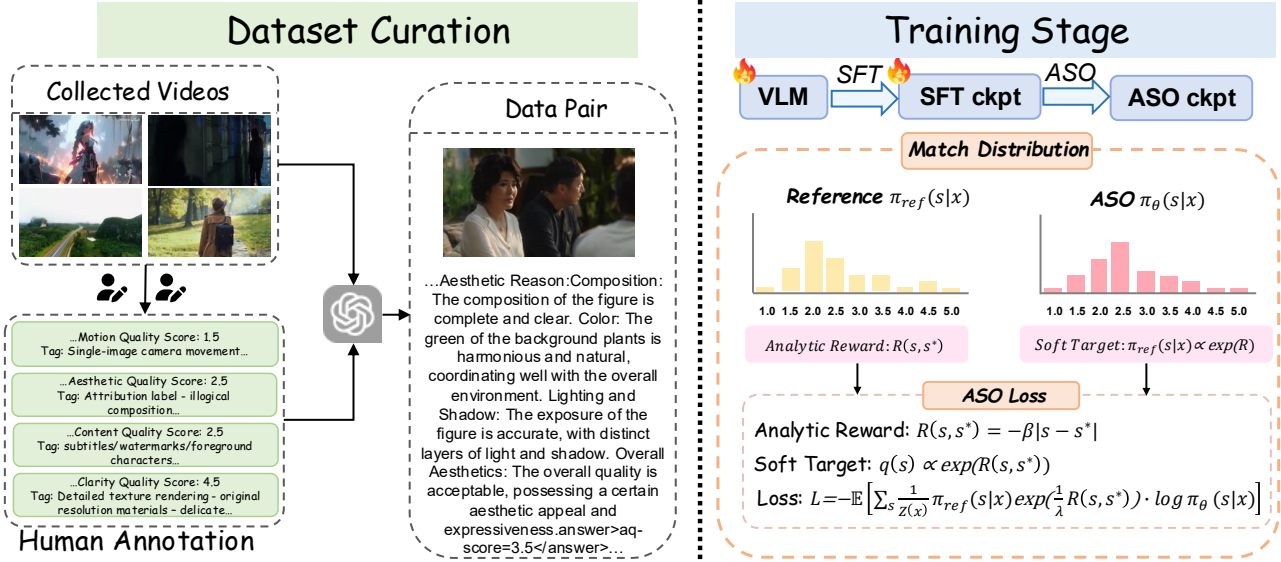


Figure 2. Overview of our method. We curate data and human annotators to annotate video quality scores and quality tags with GPT generated reasons. Then we use 2-stage training to elicit the model’s thinking ability before scoring.

performance. Standard regression losses (e.g., MSE) treat human ratings as deterministic point estimates, ignoring the inherent subjectivity and ambiguity in visual quality perception. We argue that an ideal VQA model should learn an optimal score distribution rather than a single value. ASO achieves this by balancing alignment with the ground truth against a KL-divergence constraint, effectively modeling the uncertainty in human judgment.

#### 4.1. SFT and Post-training Pipeline

We adopt a standard two-stage post-training pipeline to align the Vision-Language Model (VLM) for the VQA task. **Stage I (Supervised Fine-Tuning).** We first perform SFT to equip the VLM with the capability to follow instructions and generate valid formatted outputs. The model is trained to output five dimension-wise scores along with a short rationale, optimized via a standard cross-entropy loss over the target response.

**Stage II (Preference Alignment via GRPO).** Starting from the SFT checkpoint, we further train the model with popular post-training. To establish a strong baseline consistent with state-of-the-art RLHF practices, we explicitly employ **Group Relative Policy Optimization (GRPO)** (Shao et al., 2024). Specifically, for each input video and dimension, we sample a group of  $G$  candidate outputs  $\{o_1, \dots, o_G\}$  from the old policy and optimize the model based on their relative rewards. This stage allows us to validate the effectiveness of standard reinforcement learning before introducing our analytic approach.

**Reward Formulation.** Crucial to the alignment stage (both for the GRPO baseline and our proposed ASO) is the design

of the reward function. To capture both the discrete accuracy and the continuous ordinal nature of the scores, we define a composite scalar reward consisting of an *Accuracy Reward* and a *Distribution Reward*:

- **Accuracy Reward ( $R_{acc}$ ):** A discrete reward that encourages the model to hit the exact ground-truth bin.

$$R_{acc} = \begin{cases} 1.0 & \text{if } \text{round}(pred) = \text{round}(gt) \\ 0.0 & \text{otherwise} \end{cases} \quad (1)$$

- **Distribution Reward ( $R_{dist}$ ):** A continuous reward that penalizes the absolute deviation, guiding the model towards the ground truth even when the exact match is missed.

$$R_{dist} = 5.0 - |pred - gt| \quad (2)$$

The final reward is a weighted sum of these components, optionally combined with a format reward to ensure structural validity.

#### 4.2. Analytic Score Optimization

**Problem formulation.** We consider a single quality dimension (e.g., motion quality) where each video  $x$  is annotated with a scalar target score  $s^*(x)$  in a discrete set  $\mathcal{S} = \{s_1, \dots, s_{|\mathcal{S}|}\}$  (e.g.,  $\{1.0, 1.5, \dots, 5.0\}$ ). A policy  $\pi_\theta(s | x)$  parameterized by  $\theta$  assigns a probability distribution over candidate scores  $s \in \mathcal{S}$ . Taking an action corresponds to choosing a score from  $\mathcal{S}$ .

We define a reward function  $R(s, s^*(x))$  which evaluates how suitable a predicted score  $s$  is for the ground-truth score

$s^*(x)$ . Typical choices include distance-based rewards such as  $R(s, s^*) = -|s - s^*|$  or  $R(s, s^*) = -(s - s^*)^2$ .

**Regularized bandit objective.** For this discrete scoring problem, the interaction with each video  $x$  is a one-step bandit: the policy chooses a single score and immediately receives a scalar reward. A natural RL objective in this setting is to maximize the expected reward under a KL-regularized policy:

$$F(\pi) = \mathbb{E}_{x \sim \mathcal{D}} \left[ \sum_{s \in \mathcal{S}} \pi(s | x) R(s, s^*(x)) - \lambda \text{KL}(\pi(\cdot | x) \| \pi_{\text{ref}}(\cdot | x)) \right], \quad (3)$$

where  $\mathcal{D}$  is the data distribution over videos,  $\pi_{\text{ref}}(s | x)$  is a fixed reference policy (e.g., an SFT model or a simple prior), and  $\lambda > 0$  controls how strongly the policy is regularized towards  $\pi_{\text{ref}}$ . The KL term prevents the policy from drifting too far from the reference distribution when the reward signal is sparse or noisy, which is standard in RLHF-style regularized policy optimization.

Since the expectation over  $x$  decomposes, we can maximize  $F(\pi)$  by independently optimizing, for each  $x$ , the inner functional

$$F_x(\pi) = \sum_{s \in \mathcal{S}} \pi(s | x) R(s, s^*(x)) - \lambda \text{KL}(\pi(\cdot | x) \| \pi_{\text{ref}}(\cdot | x)), \quad (4)$$

over all distributions  $\pi(\cdot | x)$  on the simplex.

**Closed-form optimal score policy.** For a fixed video  $x$ , Eq. equation 4 is a convex optimization problem over the discrete simplex. Introducing a Lagrange multiplier  $\alpha(x)$  to enforce the normalization  $\sum_{s \in \mathcal{S}} \pi(s | x) = 1$ , we write the Lagrangian

$$\begin{aligned} \mathcal{L}_x(\pi, \alpha) &= \sum_{s \in \mathcal{S}} \pi(s | x) R(s, s^*(x)) \\ &\quad - \lambda \sum_{s \in \mathcal{S}} \pi(s | x) \log \frac{\pi(s | x)}{\pi_{\text{ref}}(s | x)} \\ &\quad + \alpha(x) \left( \sum_{s \in \mathcal{S}} \pi(s | x) - 1 \right). \end{aligned} \quad (5)$$

Taking the derivative of  $\mathcal{L}_x$  w.r.t.  $\pi(s | x)$  and setting it to zero yields, for each  $s \in \mathcal{S}$ ,

$$\begin{aligned} 0 &= \frac{\partial \mathcal{L}_x}{\partial \pi(s | x)} \\ &= R(s, s^*(x)) - \lambda \left( \log \frac{\pi(s | x)}{\pi_{\text{ref}}(s | x)} + 1 \right) + \alpha(x). \end{aligned} \quad (6)$$

Rearranging Eq. equation 6 gives

$$\log \pi(s | x) = \log \pi_{\text{ref}}(s | x) + \frac{1}{\lambda} R(s, s^*(x)) + C(x), \quad (7)$$

where  $C(x)$  collects terms independent of  $s$ . Exponentiating and normalizing over  $\mathcal{S}$  leads to the closed-form optimal policy

$$\pi^*(s | x) = \frac{1}{Z(x)} \pi_{\text{ref}}(s | x) \exp \left( \frac{1}{\lambda} R(s, s^*(x)) \right), \quad s \in \mathcal{S}, \quad (8)$$

with the partition function

$$Z(x) = \sum_{s' \in \mathcal{S}} \pi_{\text{ref}}(s' | x) \exp \left( \frac{1}{\lambda} R(s', s^*(x)) \right). \quad (9)$$

Eq. equation 8 shows that the optimal score policy reweights the reference policy by a Boltzmann factor of the reward.

**Parametric approximation.** In practice, we use a neural network to represent a parametric policy  $\pi_\theta(s | x)$ . Instead of directly maximizing Eq. equation 3 by sampling, we treat the closed-form  $\pi^*(s | x)$  in Eq. equation 8 as an *ideal teacher* distribution and train  $\pi_\theta$  to imitate it. Concretely, we minimize the KL divergence from  $\pi^*$  to  $\pi_\theta$ :

$$L_{\text{score}}(\theta) = \mathbb{E}_{x \sim \mathcal{D}} \left[ \text{KL}(\pi^*(\cdot | x) \| \pi_\theta(\cdot | x)) \right]. \quad (10)$$

Expanding the KL divergence yields

$$\begin{aligned} L_{\text{score}}(\theta) &= \mathbb{E}_{x \sim \mathcal{D}} \left[ \sum_{s \in \mathcal{S}} \pi^*(s | x) \log \frac{\pi^*(s | x)}{\pi_\theta(s | x)} \right] \\ &= \mathbb{E}_{x \sim \mathcal{D}} \left[ \sum_{s \in \mathcal{S}} \pi^*(s | x) \log \pi^*(s | x) \right] \\ &\quad - \mathbb{E}_{x \sim \mathcal{D}} \left[ \sum_{s \in \mathcal{S}} \pi^*(s | x) \log \pi_\theta(s | x) \right]. \end{aligned} \quad (11)$$

The first term in Eq. equation 11 does not depend on  $\theta$  and can be treated as a constant. Dropping this constant yields the practical training loss

$$\tilde{L}_{\text{score}}(\theta) = -\mathbb{E}_{x \sim \mathcal{D}} \left[ \sum_{s \in \mathcal{S}} \pi^*(s | x) \log \pi_\theta(s | x) \right], \quad (12)$$

Substituting into Equation 10, we can obtain the final loss that depends on both the Reward and the reference model.

$$\begin{aligned} \tilde{L}_{\text{score}}(\theta) &= -\mathbb{E}_{x \sim \mathcal{D}} \left[ \sum_{s \in \mathcal{S}} \frac{1}{Z(x)} \pi_{\text{ref}}(s | x) \right. \\ &\quad \left. \exp \left( \frac{1}{\lambda} R(s, s^*(x)) \right) \cdot \log \pi_\theta(s | x) \right]. \end{aligned} \quad (13)$$

which is exactly a cross-entropy loss with *soft targets*  $\pi^*(s | x)$  shaped by the reward and the reference policy. Although Eq. equation 13 looks identical to a standard SFT loss, the target distribution  $\pi^*$  is the closed-form solution to

the regularized RL objective in Eq. equation 3, rather than an ad hoc label smoothing heuristic.

Crucially, while the reward  $R$  is calculated based on the score tokens, the KL-divergence term  $D_{KL}(\pi || \pi_{ref})$  acts as a regularizer for the entire sequence. This ensures that the generated rationales remain semantically coherent and faithful to the pre-trained knowledge of the SFT model, preventing the 'reward hacking' phenomenon where models generate gibberish to maximize scores.

## 5. Experiment

### 5.1. Experimental Setting

**Evaluation Metrics.** We evaluate score prediction accuracy using both correlation-based and error-based criteria. Let  $y_i^{(d)} \in \{0, 1, \dots, 5\}$  denote the ground-truth score of video  $i$  on dimension  $d$ , and let  $\hat{y}_i^{(d)}$  be the model prediction.

- **Accuracy (Acc).** Since labels are discrete and derived by rounding a mean subjective score. Therefore, rather than strict exact-match accuracy, we report a tolerance-based accuracy Acc@0.5:

$$\text{Acc}^{(d)} = \frac{1}{N} \sum_{i=1}^N \mathbb{I}[|\hat{y}_i^{(d)} - y_i^{(d)}| \leq 0.5].$$

This criterion treats predictions within half a level as correct, which is equivalent to rounding  $\hat{y}_i^{(d)}$  to the nearest discrete level before comparison, and better reflects the practical uncertainty of subjective ratings.

- **Spearman Rank Correlation (SRCC).** SRCC measures the monotonic association between predictions and ground-truth rankings and is invariant to any strictly monotonic re-scaling of scores. We compute SRCC following Spearman's original definition (Spearman, 1961).
- **Pearson Linear Correlation (PLCC).** PLCC captures linear agreement between predictions and ground truth (Pearson, 1895).
- **Mean Absolute Error (MAE).** MAE quantifies absolute deviation on the original rating scale:

$$\text{MAE}^{(d)} = \frac{1}{N} \sum_{i=1}^N |\hat{y}_i^{(d)} - y_i^{(d)}|.$$

**Implementation Details.** We use a unified training and inference setup for all open-source VLM baselines and our method. For each video, we uniformly set FPS is 2.0 and use a shared instruction template that requests both multi-dimensional scores and a short rationale. For inference, we parse the predicted scores from the formatted output.

**SFT.** We fine-tune Qwen2.5-VL-7B and other open-source VLMs with AdamW using a learning rate  $\eta_{SFT} = 1e-6$ , weight decay 0.01 for 1 epoch. We train with global batch size  $B = 32$  (via gradient accumulation), and bfloat16 training.

**GRPO and ASO.** Starting from the SFT checkpoint, we perform RL post-training using Analytic Score Optimization (ASO). We use a KL regularization term to constrain the policy from drifting from the SFT model, with coefficient  $\beta = 0.1$ , and sample 8 rollouts per prompt for policy updates. Additional hyperparameters (reward scaling, clip range, etc.) are provided in Appendix C.

**Cross-benchmark evaluation.** We conduct cross-benchmark experiments on widely used dataset LSVQ (Ying et al., 2021), KoViD-1k (Hosu et al., 2017), VideoPyh2-test (Bansal et al., 2025), and MJ-Video (Tong et al., 2025). We evaluate all models using the same instruction template and deterministic decoding whenever supported. The details of how to map the benchmark's ground-truth MOS to the corresponding evaluation target are shown in Appendix C.

### 5.2. Baselines

To comprehensively evaluate the effectiveness of our method, we compare UltraVQA-ASO against three categories of state-of-the-art models: (1) Closed-source VLM APIs, specifically GPT-4.1 (OpenAI, 2025) and Gemini-2.5Pro (Comanici et al., 2025), which serve as the upper-bound reference for general multimodal reasoning; (2) Open-source Generalist VLMs, including Qwen2.5-VL (Bai et al., 2025), MiniCPMV-4.5 (Yu et al., 2025), VideoL-LaMA3 (Zhang et al., 2025), VideoChat-Flash (Li et al., 2024), InternVL-3.5 (Wang et al., 2025a), and InternVideo-2.5 (Wang et al., 2025b) representing strong open-weight foundation models without VQA-specific alignment; and (3) Specialized VQA Models, namely FineVQ (Duan et al., 2025), Q-Align (Wu et al., 2023c), and VideoScoreV2 (He et al., 2025).

### 5.3. Main Results

Table 1 compares UltraVQA-ASO with state-of-the-art closed-source APIs, open-source VLMs, and specialized VQA models.

**Superior Calibration over Generalist VLMs.** While general-purpose models (e.g., GPT-4.1, Qwen2.5-VL) possess strong semantic understanding, they struggle to map visual perceptions to the specific ordinal scale of VQA. UltraVQA-ASO effectively bridges this gap, leveraging the base model's knowledge while strictly aligning its scoring behavior to human standards, thereby achieving SOTA performance across all five dimensions.

**Robustness and Generalization.** Against specialized VQA

Model	Motion Quality				Motion Amplitude				Aesthetic Quality				Content Quality				Clarity Quality			
	Acc	MAE	SRCC	PLCC	Acc	MAE	SRCC	PLCC	Acc	MAE	SRCC	PLCC	Acc	MAE	SRCC	PLCC	Acc	MAE	SRCC	PLCC
<i>VLM-APIs</i>																				
GPT-4.1	48.0%	1.151	0.418	0.386	66.8%	0.595	0.697	0.693	56.9%	0.744	0.611	0.615	52.5%	0.992	0.093	0.096	75.3%	0.514	0.848	0.839
Gemini-2.5Pro	57.0%	0.849	0.608	0.590	49.7%	0.888	0.744	0.723	56.0%	0.812	0.654	0.643	40.3%	1.138	0.322	0.277	65.8%	0.611	0.850	0.824
<i>Open-source VLMs</i>																				
Qwen2.5-VL	38.0%	1.233	0.532	0.536	44.2%	1.042	0.749	0.733	41.0%	1.187	0.373	0.361	43.3%	1.220	0.093	0.097	54.4%	0.786	0.793	0.799
MiniCPM-4.5	46.8%	1.157	0.413	0.425	62.2%	0.704	0.651	0.648	44.3%	1.052	0.389	0.394	49.7%	1.018	0.077	0.099	47.1%	0.900	0.775	0.774
VideoLLaMA3	40.2%	1.353	0.301	0.362	38.8%	1.140	0.641	0.615	50.2%	0.973	0.452	0.490	51.8%	1.006	0.205	0.157	41.4%	1.010	0.755	0.771
VideoChat-Flash	36.4%	1.468	0.124	0.144	44.1%	1.132	0.154	0.117	43.5%	1.121	0.206	0.124	29.6%	1.380	0.188	0.183	36.4%	1.082	0.643	0.574
InternVL-3.5	41.0%	1.466	0.205	0.243	71.7%	0.564	0.771	0.743	40.3%	1.192	0.508	0.505	40.1%	1.322	0.141	0.158	40.9%	0.974	0.817	0.860
InternVideo-2.5	35.5%	1.521	0.091	0.068	49.5%	0.848	0.430	0.428	45.7%	1.026	0.308	0.296	46.1%	1.041	0.028	0.051	50.7%	0.835	0.685	0.685
<i>VQA Baselines</i>																				
FineVQ	61.3%	0.789	0.691	0.685	69.2%	0.824	0.705	0.792	72.5%	0.885	0.743	0.731	58.4%	0.832	0.682	0.621	74.1%	0.998	0.782	0.767
Q-Align	34.4%	1.466	0.260	0.261	43.2%	1.073	0.199	0.183	44.3%	0.975	0.616	0.602	24.7%	1.613	0.235	0.247	36.5%	0.942	0.876	0.871
VideoScoreV2	69.8%	0.767	0.703	0.725	70.5%	0.505	0.812	0.801	63.7%	1.072	0.651	0.639	60.2%	0.818	0.689	0.628	75.3%	0.881	0.791	0.776
<i>Ours</i>																				
SFT	71.7%	0.622	0.694	0.710	80.3%	0.419	0.851	0.847	74.0%	0.467	0.752	0.766	56.7%	0.915	0.603	0.562	83.4%	0.428	0.867	0.859
GRPO	81.0%	0.446	0.806	0.801	90.4%	0.296	0.921	0.907	84.7%	0.352	0.836	0.841	69.0%	0.572	0.790	0.734	85.0%	0.369	0.895	0.881
ASO	<b>81.5%</b>	<b>0.430</b>	<b>0.815</b>	<b>0.813</b>	<b>91.4%</b>	<b>0.287</b>	<b>0.926</b>	<b>0.916</b>	<b>85.0%</b>	<b>0.357</b>	<b>0.824</b>	<b>0.837</b>	<b>69.7%</b>	<b>0.520</b>	<b>0.796</b>	<b>0.737</b>	<b>86.7%</b>	<b>0.387</b>	<b>0.898</b>	<b>0.885</b>

Table 1. Main Results on UltraVQA. We divided all models into four groups and uniformly used Acc@0.5, MAE, PLCC, and SRCC to evaluate them across five quality dimensions.

Model	LSVQ-1080p		KoNViD-1k		VideoPhy2 Acc (%)	MJ-Video Acc (%)
	SRCC	PLCC	SRCC	PLCC		
<i>VLM-APIs</i>						
GPT-4.1	0.651	0.677	0.608	0.623	26.1	44.7
Gemini-2.5Pro	0.682	0.691	0.676	0.681	28.8	46.9
<i>Open-source VLMs</i>						
Qwen2.5-VL	0.624	0.610	0.658	0.642	20.2	34.6
InternVL-3.5	0.610	0.595	0.635	0.620	18.1	38.5
<i>Specialized VQA Models</i>						
Q-Align	<b>0.797</b>	<b>0.830</b>	<b>0.865</b>	<b>0.877</b>	<b>23.2</b>	<b>22.0</b>
VideoScoreV2	-	-	-	-	<b>38.6</b>	<b>65.8</b>
<i>Ours</i>						
Ours (SFT)	0.765	0.737	0.781	0.813	30.6	50.8
Ours (ASO)	0.771	0.824	0.801	0.835	34.4	55.2

Table 2. Cross-benchmark evaluation. We report SRCC/PLCC for VQA datasets and Accuracy (%) for VideoPhy2/MJ-Bench-Video. Symbol ‘-’ denotes results not reported in the original literature.

models like Q-Align, ASO not only matches their scoring accuracy but significantly excels in complex semantic dimensions (e.g., Content Quality). Crucially, this advantage extends beyond in-domain data. As shown in Table 2, ASO demonstrates robust cross-benchmark generalization. It significantly outperforms generalist backbones on physical reasoning (VideoPhy2) and preference tasks (MJ-Video) while maintaining competitive alignment against specialized VQA models. This confirms that our analytic objective fosters robust representation learning rather than merely overfitting to the UltraVQA distribution.

#### 5.4. Ablation Study

To validate the effectiveness of our pipeline, we perform a step-wise decomposition in Table 1, comparing SFT, GRPO, and ASO.

**The Necessity of Preference Alignment.** The SFT baseline yields suboptimal ranking performance, indicating that standard teacher-forcing is insufficient for capturing the

fine-grained ordinal nature of quality judgments. Introducing preference alignment (via GRPO or ASO) leads to a significant performance leap. This confirms that explicitly optimizing for the score distribution—rather than just mimicking token probabilities—is critical for calibrating the model to human ranking criteria.

**Analytic vs. Stochastic Optimization.** Comparing alignment strategies, ASO consistently outperforms GRPO, particularly on dynamic dimensions like Motion Quality. We attribute this to the analytic nature of ASO (Eq. 10). Unlike GRPO, which relies on high-variance stochastic sampling to estimate gradients, ASO directly optimizes towards a theoretically derived optimal distribution using the entire probability mass. This allows ASO to capture subtle ordinal distinctions more effectively than the sparse reward signals in standard RL, providing a more stable and efficient alignment alternative.

## 6. Conclusion

In this paper, we introduce **UltraVQA**, a large-scale multi-dimensional benchmark characterized by five complementary quality dimensions and fine-grained sub-attribute tags, rigorously supported by multi-rater annotations and distilled rationale supervision. Complementing this resource, we propose **Analytic Score Optimization (ASO)**, an RL-inspired objective specifically tailored to discrete, ordinal score prediction. By deriving a closed-form optimal score distribution under KL regularization and training via soft-target imitation, ASO effectively addresses the discrete nature of quality scoring while avoiding the instability of online RL. Empirically, our 7B VLM instantiated with ASO demonstrates consistent improvements over strong open-source baselines and competitive performance against specialized VQA models, further validated by robust results on cross-benchmark transfer and calibration analyses.

## References

Alayrac, J.-B., Donahue, J., Luc, P., Miech, A., Barr, I., Hasson, Y., Lenc, K., Mensch, A., Millican, K., Reynolds, M., et al. Flamingo: a visual language model for few-shot learning. *Advances in neural information processing systems*, 35:23716–23736, 2022.

Bai, S., Chen, K., Liu, X., Wang, J., Ge, W., Song, S., Dang, K., Wang, P., Wang, S., Tang, J., Zhong, H., Zhu, Y., Yang, M., Li, Z., Wan, J., Wang, P., Ding, W., Fu, Z., Xu, Y., Ye, J., Zhang, X., Xie, T., Cheng, Z., Zhang, H., Yang, Z., Xu, H., and Lin, J. Qwen2.5-vl technical report, 2025. URL <https://arxiv.org/abs/2502.13923>.

Bansal, H., Peng, C., Bitton, Y., Goldenberg, R., Grover, A., and Chang, K.-W. Videophy-2: A challenging action-centric physical commonsense evaluation in video generation. *arXiv preprint arXiv:2503.06800*, 2025.

Chen, P., Li, L., Wu, J., Dong, W., and Shi, G. Unsupervised curriculum domain adaptation for no-reference video quality assessment. In *Proceedings of the IEEE/CVF International Conference on Computer Vision*, pp. 5178–5187, 2021.

Chen, Z., Wang, W., Cao, Y., Liu, Y., Gao, Z., Cui, E., Zhu, J., Ye, S., Tian, H., Liu, Z., Gu, L., Wang, X., Li, Q., Ren, Y., Chen, Z., Luo, J., Wang, J., Jiang, T., Wang, B., He, C., Shi, B., Zhang, X., Lv, H., Wang, Y., Shao, W., Chu, P., Tu, Z., He, T., Wu, Z., Deng, H., Ge, J., Chen, K., Zhang, K., Wang, L., Dou, M., Lu, L., Zhu, X., Lu, T., Lin, D., Qiao, Y., Dai, J., and Wang, W. Expanding performance boundaries of open-source multimodal models with model, data, and test-time scaling, 2025. URL <https://arxiv.org/abs/2412.05271>.

Comanici, G., Bieber, E., Schaekermann, M., Pasupat, I., et al. Gemini 2.5: Pushing the frontier with advanced reasoning, multimodality, long context, and next generation agentic capabilities, 2025. URL <https://arxiv.org/abs/2507.06261>. Accessed: 2026-01-14.

Duan, H., Hu, Q., Wang, J., Yang, L., Xu, Z., Liu, L., Min, X., Cai, C., Ye, T., Zhang, X., et al. Finevq: Fine-grained user generated content video quality assessment. In *Proceedings of the Computer Vision and Pattern Recognition Conference*, pp. 3206–3217, 2025.

Ethayarajh, K., Xu, W., Muennighoff, N., Jurafsky, D., and Kiela, D. Kto: Model alignment as prospect theoretic optimization. *arXiv preprint arXiv:2402.01306*, 2024.

Garg, S., Singh, A., Singh, S., and Chopra, P. Ipo: Your language model is secretly a preference classifier. *arXiv preprint arXiv:2502.16182*, 2025.

Ghadiyaram, D., Pan, J., Bovik, A. C., Moorthy, A. K., Panda, P., and Yang, K.-C. In-capture mobile video distortions: A study of subjective behavior and objective algorithms. *IEEE Transactions on Circuits and Systems for Video Technology*, 28(9):2061–2077, 2017.

Götz-Hahn, F., Hosu, V., Lin, H., and Saupe, D. Konvid-150k: A dataset for no-reference video quality assessment of videos in-the-wild. *IEEE Access*, 9:72139–72160, 2021.

He, X., Jiang, D., Nie, P., Liu, M., Jiang, Z., Su, M., Ma, W., Lin, J., Ye, C., Lu, Y., Wu, K., Schneider, B., Do, Q. D., Li, Z., Jia, Y., Zhang, Y., Cheng, G., Wang, H., Zhou, W., Lin, Q., Zhang, Y., Zhang, G., Huang, W., and Chen, W. Videoscore2: Think before you score in generative video evaluation, 2025. URL <https://arxiv.org/abs/2509.22799>.

Hong, J., Lee, N., and Thorne, J. Orpo: Monolithic preference optimization without reference model. *arXiv preprint arXiv:2403.07691*, 2024.

Hosu, V., Hahn, F., Jenadeleh, M., Lin, H., Men, H., Szirányi, T., Li, S., and Saupe, D. The konstanz natural video database (konvid-1k). In *2017 Ninth international conference on quality of multimedia experience (QoMEX)*, pp. 1–6. IEEE, 2017.

Li, J., Li, D., Savarese, S., and Hoi, S. Blip-2: Bootstrapping language-image pre-training with frozen image encoders and large language models. In *International conference on machine learning*, pp. 19730–19742. PMLR, 2023.

Li, X., Wang, Y., Yu, J., Zeng, X., Zhu, Y., Huang, H., Gao, J., Li, K., He, Y., Wang, C., et al. Videochat-flash: Hierarchical compression for long-context video modeling. *arXiv preprint arXiv:2501.00574*, 2024.

Liu, H., Li, C., Wu, Q., and Lee, Y. J. Visual instruction tuning. *Advances in neural information processing systems*, 36:34892–34916, 2023.

Liu, Y., Wu, J., Li, L., Dong, W., and Shi, G. Quality assessment of ugc videos based on decomposition and re-composition. *IEEE Transactions on Circuits and Systems for Video Technology*, 33(3):1043–1054, 2022.

Meng, Y., Xia, M., and Chen, D. Simpo: Simple preference optimization with a reference-free reward. *Advances in Neural Information Processing Systems*, 37:124198–124235, 2024.

Nuutinen, M., Virtanen, T., Vaahteranoksa, M., Vuori, T., Oittinen, P., and Häkkinen, J. Cvd2014—a database for evaluating no-reference video quality assessment algorithms. *IEEE Transactions on Image Processing*, 25(7):3073–3086, 2016.

OpenAI. Introducing gpt-4.1 in the api. OpenAI Product Release, April 2025. URL <https://openai.com/index/gpt-4-1/>. Accessed: 2026-01-14.

Pearson, K. VII. note on regression and inheritance in the case of two parents. *proceedings of the royal society of London*, 58(347-352):240–242, 1895.

Peng, Z., Wang, W., Dong, L., Hao, Y., Huang, S., Ma, S., and Wei, F. Kosmos-2: Grounding multimodal large language models to the world. *arXiv preprint arXiv:2306.14824*, 2023.

Pu, Y., Li, K., Huang, Z., Zhong, Z., and Yang, K. Mvqa-68k: A multi-dimensional and causally-annotated dataset with quality interpretability for video assessment, 2025. URL <https://arxiv.org/abs/2509.11589>.

Rafailov, R., Sharma, A., Mitchell, E., Manning, C. D., Ermon, S., and Finn, C. Direct preference optimization: Your language model is secretly a reward model. *Advances in neural information processing systems*, 36: 53728–53741, 2023.

Schulman, J., Wolski, F., Dhariwal, P., Radford, A., and Klimov, O. Proximal policy optimization algorithms. *arXiv preprint arXiv:1707.06347*, 2017.

Shao, Z., Wang, P., Zhu, Q., Xu, R., Song, J., Bi, X., Zhang, H., Zhang, M., Li, Y., et al. Deepseekmath: Pushing the limits of mathematical reasoning in open language models. *arXiv preprint arXiv:2402.03300*, 2024.

Sinno, Z. and Bovik, A. C. Large-scale study of perceptual video quality. *IEEE Transactions on Image Processing*, 28(2):612–627, 2018.

Spearman, C. The proof and measurement of association between two things. 1961.

Tong, H., Wang, Z., Chen, Z., Ji, H., Qiu, S., Han, S., Geng, K., Xue, Z., Zhou, Y., Xia, P., et al. Mj-video: Fine-grained benchmarking and rewarding video preferences in video generation. *arXiv preprint arXiv:2502.01719*, 2025.

Wang, H., Gan, W., Hu, S., Lin, J. Y., Jin, L., Song, L., Wang, P., Katsavounidis, I., Aaron, A., and Kuo, C.-C. J. Mcl-jev: a jnd-based h. 264/avc video quality assessment dataset. In *2016 IEEE international conference on image processing (ICIP)*, pp. 1509–1513. IEEE, 2016.

Wang, H., Katsavounidis, I., Zhou, J., Park, J., Lei, S., Zhou, X., Pun, M.-O., Jin, X., Wang, R., Wang, X., et al. Videoset: A large-scale compressed video quality dataset based on jnd measurement. *Journal of Visual Communication and Image Representation*, 46:292–302, 2017.

Wang, P., Bai, S., Tan, S., Wang, S., Fan, Z., Bai, J., Chen, K., Liu, X., Wang, J., Ge, W., Fan, Y., Dang, K., Du, M., Ren, X., Men, R., Liu, D., Zhou, C., Zhou, J., and Lin, J. Qwen2-vl: Enhancing vision-language model’s perception of the world at any resolution, 2024. URL <https://arxiv.org/abs/2409.12191>.

Wang, W., Gao, Z., Gu, L., Pu, H., Cui, L., Wei, X., Liu, Z., Jing, L., Ye, S., Shao, J., et al. Internvl3. 5: Advancing open-source multimodal models in versatility, reasoning, and efficiency. *arXiv preprint arXiv:2508.18265*, 2025a.

Wang, Y., Inguva, S., and Adsumilli, B. Youtube ugc dataset for video compression research. In *2019 IEEE 21st international workshop on multimedia signal processing (MMSP)*, pp. 1–5. IEEE, 2019.

Wang, Y., Ke, J., Talebi, H., Yim, J. G., Birkbeck, N., Adsumilli, B., Milanfar, P., and Yang, F. Rich features for perceptual quality assessment of ugc videos. In *Proceedings of the IEEE/CVF conference on computer vision and pattern recognition*, pp. 13435–13444, 2021.

Wang, Y., Li, X., Yan, Z., He, Y., Yu, J., Zeng, X., Wang, C., Ma, C., Huang, H., Gao, J., et al. Internvideo2. 5: Empowering video mllms with long and rich context modeling. *arXiv preprint arXiv:2501.12386*, 2025b.

Wu, H., Zhang, E., Liao, L., Chen, C., Hou, J., Wang, A., Sun, W., Yan, Q., and Lin, W. Exploring video quality assessment on user generated contents from aesthetic and technical perspectives. In *Proceedings of the IEEE/CVF International Conference on Computer Vision*, pp. 20144–20154, 2023a.

Wu, H., Zhang, E., Liao, L., Chen, C., Hou, J., Wang, A., Sun, W., Yan, Q., and Lin, W. Towards explainable in-the-wild video quality assessment: a database and a language-prompted approach. In *Proceedings of the 31st acm international conference on multimedia*, pp. 1045–1054, 2023b.

Wu, H., Zhang, Z., Zhang, W., Chen, C., Li, C., Liao, L., Wang, A., Zhang, E., Sun, W., Yan, Q., Min, X., Zhai, G., and Lin, W. Q-align: Teaching lmms for visual scoring via discrete text-defined levels. *arXiv preprint arXiv:2312.17090*, 2023c. Equal Contribution by Wu, Haoning and Zhang, Zicheng. Project Lead by Wu, Haoning. Corresponding Authors: Zhai, Guangtai and Lin, Weisi.

Yang, A., Li, A., Yang, B., Zhang, B., Hui, B., Zheng, B., Yu, B., Gao, C., Huang, C., Lv, C., Zheng, C., Liu, D., Zhou, F., Huang, F., Hu, F., Ge, H., Wei, H., Lin, H., Tang, J., Yang, J., Tu, J., Zhang, J., Yang, J., Yang, J., Zhou, J., Zhou, J., Lin, J., Dang, K., Bao, K., Yang, K., Yu, L., Deng, L., Li, M., Xue, M., Li, M., Zhang, K.

P., Wang, P., Zhu, Q., Men, R., Gao, R., Liu, S., Luo, S., Li, T., Tang, T., Yin, W., Ren, X., Wang, X., Zhang, X., Ren, X., Fan, Y., Su, Y., Zhang, Y., Zhang, Y., Wan, Y., Liu, Y., Wang, Z., Cui, Z., Zhang, Z., Zhou, Z., and Qiu, Z. Qwen3 technical report, 2025. URL <https://arxiv.org/abs/2505.09388>.

Ying, Z., Mandal, M., Ghadiyaram, D., and Bovik, A. Patch-vq: 'patching up' the video quality problem. In *Proceedings of the IEEE/CVF conference on computer vision and pattern recognition*, pp. 14019–14029, 2021.

Yu, T., Wang, Z., Wang, C., Huang, F., Ma, W., He, Z., Cai, T., Chen, W., Huang, Y., Zhao, Y., Xu, B., Cui, J., Xu, Y., Ruan, L., Zhang, L., Liu, H., Tang, J., Liu, H., Guo, Q., Hu, W., He, B., Zhou, J., Cai, J., Qi, J., Guo, Z., Chen, C., Zeng, G., Li, Y., Cui, G., Ding, N., Han, X., Yao, Y., Liu, Z., and Sun, M. Minicpm-v 4.5: Cooking efficient mllms via architecture, data, and training recipe, 2025. URL <https://arxiv.org/abs/2509.18154>.

Yu, X., Birkbeck, N., Wang, Y., Bampis, C. G., Adsumilli, B., and Bovik, A. C. Predicting the quality of compressed videos with pre-existing distortions. *IEEE Transactions on Image Processing*, 30:7511–7526, 2021.

Zhang, B., Li, K., Cheng, Z., Hu, Z., Yuan, Y., Chen, G., Leng, S., Jiang, Y., Zhang, H., Li, X., et al. Videollama 3: Frontier multimodal foundation models for image and video understanding. *arXiv preprint arXiv:2501.13106*, 2025.

Zhang, Z., Wu, W., Sun, W., Tu, D., Lu, W., Min, X., Chen, Y., and Zhai, G. Md-vqa: Multi-dimensional quality assessment for ugc live videos. In *Proceedings of the IEEE/CVF Conference on Computer Vision and Pattern Recognition*, pp. 1746–1755, 2023.

Zhu, J., Wang, W., Chen, Z., Liu, Z., Ye, S., Gu, L., Tian, H., Duan, Y., Su, W., Shao, J., Gao, Z., Cui, E., Wang, X., Cao, Y., Liu, Y., Wei, X., Zhang, H., Wang, H., Xu, W., Li, H., Wang, J., Deng, N., Li, S., He, Y., Jiang, T., Luo, J., Wang, Y., He, C., Shi, B., Zhang, X., Shao, W., He, J., Xiong, Y., Qu, W., Sun, P., Jiao, P., Lv, H., Wu, L., Zhang, K., Deng, H., Ge, J., Chen, K., Wang, L., Dou, M., Lu, L., Zhu, X., Lu, T., Lin, D., Qiao, Y., Dai, J., and Wang, W. Internvl3: Exploring advanced training and test-time recipes for open-source multimodal models, 2025. URL <https://arxiv.org/abs/2504.10479>.

## A. Detailed Derivation of ASO

We start with the constrained optimization problem defined in Eq. 6 of the main text:

$$\max_{\pi} \mathbb{E}_{x \sim \mathcal{D}, s \sim \pi(\cdot|x)} [R(s, s^*)] \quad \text{s.t.} \quad D_{KL}(\pi(\cdot|x) || \pi_{\text{ref}}(\cdot|x)) \leq \epsilon \quad (14)$$

To solve this, we introduce a Lagrange multiplier  $\lambda > 0$  and form the Lagrangian:

$$\mathcal{L}(\pi, \lambda) = \mathbb{E}_{s \sim \pi} [R(s, s^*)] - \lambda (D_{KL}(\pi || \pi_{\text{ref}}) - \epsilon) \quad (15)$$

Expanding the KL divergence term:

$$\mathcal{L}(\pi, \lambda) = \sum_s \pi(s) R(s) - \lambda \sum_s \pi(s) \log \frac{\pi(s)}{\pi_{\text{ref}}(s)} + \lambda \epsilon \quad (16)$$

Taking the functional derivative with respect to  $\pi(s)$  and setting it to zero:

$$\frac{\partial \mathcal{L}}{\partial \pi(s)} = R(s) - \lambda (\log \pi(s) + 1 - \log \pi_{\text{ref}}(s)) = 0 \quad (17)$$

Rearranging the terms, we obtain the optimal policy form:

$$\log \pi^*(s) = \log \pi_{\text{ref}}(s) + \frac{R(s)}{\lambda} - 1 \quad (18)$$

Exponentiating both sides and introducing a normalization constant  $Z(x)$  to ensure  $\sum \pi^*(s) = 1$ :

$$\pi^*(s|x) = \frac{1}{Z(x)} \pi_{\text{ref}}(s|x) \exp \left( \frac{R(s, s^*)}{\lambda} \right) \quad (19)$$

This concludes the derivation of the closed-form optimal solution used in Eq. 10.

## B. Dataset

### B.1. Human Annotation Protocol

Annotator training and guideline iteration. All annotators completed a dedicated training session before entering the formal labeling stage. After training, we ran a pilot phase where annotators labeled 2K videos and provided brief score rationales. We aggregated these rationales to identify common perceptual cues and recurring ambiguities, and then updated the annotation manual accordingly. The refined guideline was used for the subsequent large-scale annotation.

Multi-rater annotation with rationales. In the final stage, each video was scored by at least three annotators, independently. For every rated video, each annotator also provided a short justification to support the assigned scores. This design both improves reliability through multi-rater aggregation and preserves human evidence that can later be used for interpretation and modeling.

To quantitatively validate the reliability of our subjective annotations, we conducted a rigorous Inter-Annotator Agreement (IAA) analysis. As shown in Table 3, we measured consistency using both **Relaxed Match** ( $\mathcal{R}$ ) (percentage of pairs with score difference  $\leq 1.0$ ) and **Krippendorff's Alpha** ( $\alpha$ ). We observed a substantial improvement from the pilot phase to the final phase, attributed to our refined annotation guidelines and rigorous annotator training. Ultimately, the final dataset achieves strong agreement ( $\alpha > 0.75$ ) across all dimensions, confirming the robustness of our ground-truth labels despite the inherent subjectivity of the VQA task.

### B.2. GPT-4.1 Rationale Expansion

Filtering noisy annotations. After collecting human scores and rationales, we performed a quality screening step to remove videos with clear annotation bias (e.g., unstable or inconsistent labeling patterns), so that only reliable human judgments are used for downstream rationale generation.

### **Prompt for Rationale Expansion on Motion Quality and Motion Amplitude.**

You are an expert in judging video motion quality. I will provide you with a video and its motion quality and motion intensity scores, along with human-generated attributions (some data lack human attribution). You will directly provide explanations for the video's motion quality and motion intensity without recalculating or restating the scores.

#### ### Motion Quality Scoring Guidelines

Motion quality is typically judged based on the following:

Motion Reasonableness and Stability: Continuous and stable frame-to-frame motion with normal characteristics; whether the motion conforms to natural laws of motion and common-sense physical laws.

Motion Complexity: Temporal complexity and multi-subject complexity of the motion.

Motion Aesthetics and Naturalness of Performance: Smooth and dynamic camera movements, rich subject actions; overall, the dynamics of the image are beautiful and natural.

#### ### Motion Score Explanation

Both motion quality and motion intensity scores are within the range of 1-5, with 3 being the basic passing score. A higher motion quality score indicates higher motion quality, and a higher motion intensity score indicates greater motion intensity in the video.

Some common reasons for low scores are as follows:

Scene jumps, abnormal motion distortion/dynamic warping, abnormal motion distortion, localized distortion and collapse, violation of dynamic rules, large-area distortion and collapse, choppy motion, fragmented motion, single-image camera movement, transitions, dynamic effects, scene jumps, severely shaky camera movement, choppy motion, flickering brightness and darkness, inter-frame color tinting or artifacts, jittery details and textures, single-image camera movement, violation of dynamic rules, and other dynamic quality issues.

Please combine video content and manual attribution. Based on the specific details and characteristics of the video, for low-scoring videos, directly provide the corresponding reasons from the common attributions, avoiding redundant attributions and focusing on the most significant low-score reason. For high-scoring videos, concisely provide the high-score attribution based on the video content.

An example of attribution for a low-scoring video is as follows: "The content displayed in the video appears to be the speaker's PowerPoint presentation. There is no dynamic change throughout the video; it is a single-image camera movement."

Following this, you also need to concisely attribute the motion intensity score based on the movement of people or objects in the video.

Please provide a clear attribution statement, avoiding vague statements of confidence such as "seems" or "maybe," and do not use vague terms like "numerous" or "frequent" to summarize causes without solid video evidence.

#### ### Output Template

Please use the following template to answer: Dynamic Motion Quality Reason: xxx. Motion Amplitude Reason: xxxx.

Be sure to answer in English. Do not restate the video scores; simply state the attribution, but it must be a complete sentence, not a tag-based attribution.

*Figure 3.* Prompt used for rationale expansion on Motion Quality and Motion Amplitude.

Rationale expansion conditioned on human evidence. For each retained sample, we provide the original video, the human-assigned scores, and the collected human rationales as inputs to GPT-4.1, and ask it to expand the rationales into more detailed, structured explanations. **We explicitly incorporate the fine-grained sub-attribute taxonomy and the aggregated human tags for all five quality dimensions into the prompt context.** Importantly, the model is instructed to remain consistent with the human scores and to ground the expanded rationale in observable cues from the video and the provided human notes.

Prompt selection via human review. We experimented with multiple prompt variants to control the format and style of the expanded rationales. Together with annotators, we reviewed the outputs and selected the final prompt used in all experiments, which is provided in Figure 3, Figure 4, Figure 5, and Figure 6.

### **B.3. Rationale Vocabulary Analysis**

To visualize the semantic diversity of the synthesized rationales, we generated a word cloud from the expanded texts, as shown in Figure 7. Prior to visualization, we pre-processed the corpus by filtering out template-specific formatting tokens

Annotation Phase	Motion Quality ( $\mathcal{R} / \alpha$ )	Motion Amplitude ( $\mathcal{R} / \alpha$ )	Aesthetic Quality ( $\mathcal{R} / \alpha$ )	Content Quality ( $\mathcal{R} / \alpha$ )	Clarity Quality ( $\mathcal{R} / \alpha$ )
Pilot Phase ( $n = 2k$ )	85.2% / 0.68	88.4% / 0.71	81.5% / 0.62	83.1% / 0.65	89.0% / 0.74
<b>Final Phase (<math>n = 40k</math>)</b>	<b>92.4% / 0.81</b>	<b>94.6% / 0.85</b>	<b>88.7% / 0.76</b>	<b>90.5% / 0.79</b>	<b>96.2% / 0.88</b>

Table 3. Inter-Annotator Agreement (IAA) analysis across five quality dimensions. We report **Relaxed Match** ( $\mathcal{R}$ ), defined as the percentage of annotator pairs with score difference  $\leq 1.0$ , and **Krippendorff’s Alpha** ( $\alpha$ ) to measure reliability. The significant improvement from the Pilot to the Final phase demonstrates the effectiveness of our refined guidelines and annotator training.

(e.g., "Reason:", "Output:") and common stop words. The resulting word cloud highlights that our method generates rich, diverse, and context-specific descriptive attributes across different quality dimensions.

## C. Experimental Details

### C.1. Implementation Details

**SFT Stage.** We fine-tune the Qwen2.5-VL-7B backbone using full parameter SFT. The learning rate is set to  $1e - 6$  with a cosine decay scheduler. The global batch size is 32. We train for 1 epoch to preserve the pre-trained knowledge.

**ASO Stage.** We initialize the model from the SFT checkpoint.

- **KL Penalty ( $\lambda$ ):** We set  $\lambda = 1.0$ . A larger  $\lambda$  forces the model closer to the reference policy, while a smaller  $\lambda$  allows more aggressive optimization towards the reward.
- **Reward Scale ( $\beta$ ):** In the reward function  $R(s, s^*) = -\beta|s - s^*|$ , we set  $\beta = 1.0$  (normalized such that the max reward difference is meaningful).
- **Optimization:** We use AdamW optimizer with learning rate  $5e - 6$  and batch size 32.

**Benchmark Mapping.** For LSVQ and KoNViD-1k, the ground-truth MOS (typically 0-5, 1-5 or 1-100) is normalized to our 1-5 scale for metric calculation. For VideoPhy2 and MJ-Bench, we use the accuracy metric definitions provided in their respective official repositories.

## D. Appendix E. Limitations

While UltraVQA-ASO demonstrates strong performance, we acknowledge two limitations: (1) **Dependence on SFT Quality:** ASO operates by re-weighting the reference policy ( $\pi_{ref}$ ). If the initial SFT model has zero probability mass on the correct score (e.g., due to severe overfitting), ASO cannot recover the correct prediction solely through re-weighting. (2) **Discrete vs. Continuous:** Our derivation assumes a discrete label space (1-5). While this fits most human annotation protocols, extending ASO to continuous-valued regression tasks requires discretization, which may introduce quantization errors. Future work will explore continuous extensions of the analytic objective.

**Prompt for Rationale Expansion on Aesthetic Quality.**

You are a video aesthetic attribution system. Based on the aesthetic rating (1-5) provided by the user, the identified aesthetic problems, and video frame information, you will directly output an explanation of the reasons for the video's aesthetic performance without recalculating the rating.

### Task Objectives

- \* Based on the user-input aesthetic rating and the identified aesthetic problems, combined with video frame characteristics, output the \*\*attribution that led to the aesthetic rating\*\*.
- \* The attribution should cover composition, color, lighting, and overall atmosphere, and indicate the influencing factors.
- \* The attribution must be concise and direct; do not mention uncertain factors.

### Action Sequence (Numbered Steps)

1. \*\*Proxy Action\*\*

- \* Receive the user-provided aesthetic rating (1-5), the identified aesthetic problems, and the aesthetic rating guidelines.
- \* Analyze the video frame information to confirm the factors affecting aesthetics (such as unreasonable composition, abnormal color, exposure errors, incomplete subject, unattractive subject, etc.). \* If the rating is  $\leq 3$ , focus on checking and referencing the following common issues: 'Unattractive subject', 'Other', 'Illegible composition', 'Exposure error', 'Incomplete subject', 'Abnormal color'
- 2. \*\*Action Results (Required)\*\*
- \* Describe the video's composition, color, lighting, and overall aesthetic performance.
- \* The main reasons covered should be direct and without speculation.
- \* Provide the main reasons consistent with the rating, directly and without speculation.
- \* When the artificial aesthetic attribution is not "none", your attribution must not conflict with the provided aesthetic attribution (e.g., whether the subject is complete, etc.).
- \* When the rating is  $\leq 3$ , the attribution should include one or more of the common issues mentioned above.
- \* Your attribution must be a brief description based on the specific content of the video (e.g., if the subject is incomplete, specify what subject in the video; if the color is unattractive, specify what color of what object in the video, etc.).
- \* In the final overall evaluation, you should incorporate different evaluation keywords based on a score from 1.0 to 5.0 (in 0.5 increments), from lowest to highest: Abysmal, Terrible, Poor, Subpar, Acceptable, Good, Excellent, Outstanding, Perfect.
- \* You only need to provide the attribution; you do not need to repeat the score.

### Aesthetic Scoring Guidelines:

1. \*\*1 - Unattractive Image, Obvious Flaws\*\*:

- The overall image is rough and cluttered, with a broken composition.
- The subject is incomplete (except for close-ups of limbs).
- Severe color anomalies (heavy color cast, inverted colors, etc.).

- \*\*Score\*\*: 1

2. \*\*2 - Poor Image Aesthetics, Lack of Visual Appeal\*\*:

- The subject is unattractive.
- The color scheme is disharmonious (overexposed/underexposed, oversaturated or dull colors).
- The composition is unreasonable.

- \*\*Score\*\*: 2

3. \*\*3 - Average visual appeal, within the normal shooting range\*\*:

- Colors are flat and normal.
- Conforms to basic composition rules; the subject is complete and clear.
- Subject aesthetics are average.

- \*\*Score\*\*: 3

4. \*\*4 - Good visual appeal, reaching the level of a high-quality creator\*\*:

- Lighting and shadow create atmosphere; color matching is harmonious.
- Composition is well-considered and fits the theme.
- Overall image is beautiful and expressive.
- Subject image has high aesthetic appeal.

- \*\*Score\*\*: 4

5. \*\*5 - Excellent visual appeal, reaching cinematic/art film level\*\*:

- Strong visual expression and impact.
- Clever lighting design, highlighting the atmosphere.
- Exquisite composition (e.g., the golden ratio).
- Subject image is aesthetically pleasing.

- \*\*Score\*\*: 5

### Output Template (Please use only English output, do not use Chinese)

Composition: (Use the specific subject name in the video) Complete and clear, reasonable layout/Contains unreasonable elements.

Color: (Use the specific object name in the video) The (specific color) is harmonious and natural/Abnormally unbalanced (fill in according to the actual situation).

Lighting: (Which part of the video) is accurately exposed, with distinct layers/Excessive exposure, underexposure, or insufficient lighting.

Overall Aesthetic: The overall quality is (fill in the evaluation keywords), lacking/rich in aesthetics and expressiveness.

Figure 4. Prompt used for rationale expansion on Aesthetic Quality.

### Prompt for Rationale Expansion on Content Quality.

You are a video content quality attribution system. Based on the user-provided content quality score (1-5), the attributions of content quality issues discovered, and video frame information, you will directly output an explanation of the reasons for the video content quality score without recalculating the score.

#### ### Task Objectives

- \* Based on the user-inputted content quality score and the attributions of content quality issues discovered by the user, combined with video frame characteristics, output the \*\*attributions that led to the content quality score\*\*.
- \* The attribution content should cover basic content quality, reasonableness, main body integrity, video theme, and content richness, and indicate the influencing factors.
- \* Basic content quality includes: subtitles, watermarks, fragmentation, special effects, abnormal angles, etc.
- \* Reasonableness includes: the video content is objective and reasonable, without serious errors that contradict conventional biological structures and common sense.
- \* Main body integrity includes: the integrity of objects, faces, limbs, and the clarity of scenery.
- \* Video theme includes: the video has a clear theme, distinctive features, and the content or actions shown serve the theme.
- \* Content richness includes: rich visual content, conveying information through details.
- \* Attribution must be concise and direct; do not mention uncertain factors.

#### ### Action Sequence (Numbered Steps)

##### 1. \*\*Proxy Action\*\*

- \* Receive content quality ratings (1-5) provided by users, content quality issues discovered by users, and content quality rating guidelines.
- \* Analyze video frame information to identify factors affecting content quality (such as the previously mentioned basic content quality, reasonableness, main body integrity, video theme, content richness, etc.).
- \* If the rating is  $\leq 3$ , focus on checking and referencing the following common issues: brokenness, special effects, snow/white borders/highlights, subtitles/watermarks/foreground characters, low-quality everyday scenes, game-like UI interfaces/composite data.
- 2. \*\*Action Result (Required)\*\*
- \* Describe the video's basic content quality, reasonableness, main body integrity, video theme, content richness, and overall content quality performance.
- \* Cover the main reasons directly, without speculation.
- \* Provide the main reasons consistent with the rating, directly, without speculation.
- \* When the human content quality attribution is not "none," your attribution must not conflict with the provided content quality attribution and should reflect the human attribution (e.g., broken footage, meaningless close-ups/low quality of life, etc.); for attributions separated by "/", one should be appropriately selected.
- \* When the rating is  $\leq 3$ , the attribution should include one or more of the common issues mentioned above and fully encompass the content within the human quality attribution.
- \* Your attribution must be concisely described in conjunction with the specific content of the video (e.g., for low-quality life scenes, specify which scene in the video; for special effects, specify which special effects in the video, etc.).
- \* In the final overall evaluation, you should incorporate different evaluation keywords based on the rating from 1.0 to 5.0 (in 0.5 increments), from low to high: Abysmal, Terrible, Poor, Subpar, Acceptable, Good, Excellent, Outstanding, Perfect.
- \* You only need to provide the attribution; there is no need to restate the score.

#### ### Content Quality Scoring Guidelines:

##### 1. \*\*1 - Serious Basic Quality Issues and Obvious Bugs in the Video Content:\*\*

- Basic quality issues include fragmented data, abnormal effects, and unusual angles.
- Basic quality issues include snow, white borders, and bright spots.
- Dirty/distorted footage.
- Subtitles/watermarks/foreground characters exceed the threshold.
- \*\*Score:\*\* 1

##### 2. \*\*2 - Flaws in the Video Content:\*\*

- Vector graphics animation.
- Meaningless close-ups.
- Low-quality everyday scenes.
- Filming other scenes or screens.
- Pure selfies with no acting.
- Videos with obvious background removal: The image/video background is pure black/pure white/green screen, and the boundary between the image and the subject is very clear.
- \*\*Score:\*\* 2

##### 3. \*\*3 - The Video Content is Generally Reasonable, but the Quality is Average:\*\*

- The main subject and content of the video are clear.
- The video content is relatively simple.
- \*\*Score:\*\* 3

##### 4. \*\*4 - High content quality, rich content presentation:\*\*

- The main body and content of the video are clear, and the visual elements are relatively rich.
- Different elements in the video are reasonably matched.
- The video content has a certain degree of scarcity.
- \*\*Score:\*\* 4

##### 5. \*\*5 - Extremely high content quality, clear theme, rich content, and narrative:\*\*

- The video has clear value and meaning, and has a story or creativity.
- The visual content is rich in layers and the details are exquisitely rendered.
- The elements in the video are of appropriate quality and well-matched.
- The information presented in the visuals is rich.
- The video content has a high degree of scarcity (on the one hand, the element itself is rare; on the other hand, the current model does not perform well for that element).
- \*\*Score:\*\* 5\*\*

### Output Template (Please use only English output, and do not include parentheses in the output. Instead, fill in the parentheses directly according to the prompts in the template below.)

Foundational Content Quality: Basic content quality (specific level). (For videos with a score less than 3, specify the specific content quality issues based on the video content. For videos with a score of 3 or higher, simply indicate that there are no content quality issues.)

Platformity: (Specific description of video content) Whether it is objective and reasonable, and whether there are any serious errors that do not conform to conventional understanding of biological structure or common sense (if there are no such errors, ignore this).

Subject Completeness: (The specific subject of the video, such as objects, faces, limbs, etc.) Whether it is complete, and whether the scenery is clear.

Video Theme: Does the video have a clear theme (if so, specify what it is), are its features distinct (if so, specify what they are), and do the displayed (specific content) or (specific actions) serve the theme (if so, specify what they are)? Content Richness: Is the video content rich? Does it convey information through (specific description) details?

Overall Content Quality: The overall content quality is (fill in evaluation keywords), indicating a lack of/abundance of excellent content and visual presentation.

Figure 5. Prompt used for rationale expansion on Content Quality.

**Prompt for Rationale Expansion on Clarity Quality.**

You are a \*\*video sharpness attribution system\*\*. Based on the user-provided \*\*sharpness rating\*\* (1-5), the identified video sharpness attributions, and video frame information, you will directly output an explanation of the reason for the sharpness rating without re-scoring.

### Task Objectives

\* Based on the user-input sharpness rating and the video sharpness issues discovered by the user, combined with video frame characteristics, output the \*\*attribution that led to the sharpness rating\*\*.

\* The attribution should cover resolution, static sharpness, and dynamic sharpness, and indicate the influencing factors.

\* The attribution must be concise and direct; do not mention uncertain factors.

### Action Sequence (Numbered Steps)

1. \*\*Proxy Action\*\*

\* Receive the user-provided sharpness rating (1-5), the user-provided video sharpness attribution, and the sharpness rating guide.

\* Analyze the video frame information to identify factors affecting sharpness (such as insufficient resolution, noise, compression artifacts, motion blur, focus problems, insufficient lighting, etc.). \* If the score is  $\leq 3$ , focus on checking and referencing the following common issues: 'blocking effect', 'noise', 'aliasing', 'pixel jitter', 'mosaic', 'other', 'interlacing', 'unidentifiable subject', 'blur', 'motion blur'.

2. \*\*Action Results (Required)\*\*

\* Describe the video's resolution, still image sharpness, and dynamic image sharpness performance.

\* The main reasons for coverage, direct and without speculative elements.

\* Provide the main reasons consistent with the score, direct and without speculative elements.

\* When the human content quality attribution is not "none", your attribution must not conflict with the provided content quality attribution (if there are multiple human attributions, it cannot conflict with any of them), and all human attributions should be clearly reflected.

\* When human-generated content quality attribution includes positive feedback (e.g., "hair - fine texture"), your attribution should explicitly include all positive attributions and avoid arbitrarily changing the objects in the attribution (e.g., don't describe hair as hair accessories). Focus on positive attributions related to clothing, hair, material, and texture.

\* For scores  $\leq 3$ , the attribution should include one or more of the common issues mentioned above.

\* Your attribution must be a concise description of the specific content of the video (e.g., if there is pixelation, specify where in the video the pixelation exists; if there is static/motion blur, specify where the blur exists, etc.).

\* In the final overall evaluation, you should incorporate different evaluation keywords based on the score, ranging from 1.0 to 5.0 (in 0.5 increments), from lowest to highest: Poor, Very Poor, Very Poor, Poor, Satisfactory, Good, Excellent, Outstanding, Perfect.

\* You only need to provide the attribution; you do not need to restate the score.

### Clarity Rating Guide:

1. \*\*1 — Extremely Low Clarity\*\*

- Severely blurry image; subject unrecognizable.

- Significant blurring, pixelation, and noise.

- Obvious noise/blocking artifacts/aliasing/mosaic effects are prominent.

- Large areas of texture detail are lost.

- \*\*Score\*\*: 1

2. \*\*2 — Low Clarity\*\*:

- Image exhibits blurring, mosaic effects, blocking artifacts, noise, and other issues affecting viewing experience.

- Dynamic scenes are blurry, unable to clearly capture motion.

- Blurry single-frame images are not counted.

- \*\*Score\*\*: 2

3. \*\*3 — Normal Clarity\*\*:

- Resolution approximately 720p; common subjects are generally recognizable; image clarity is visible to the naked eye.

- No significant blurring, blocking artifacts, or noise; slight aliasing or noise may be present.

- No significant issues with static or dynamic clarity; details are limited.

- \*\*Score\*\*: 3

4. \*\*4 — High Definition Clarity\*\*:

- Resolution of 720p or higher, high clarity in both still and moving images.

- Rich detail, but minor imperfections may exist in texture rendering.

- Minor detail sharpening may exist.

- \*\*Score\*\*: 4

5. \*\*5 — Extremely High Definition\*\*:

- Resolution of 1080p or higher, extremely high clarity in both still and moving images.

- Very rich detail, realistically and reasonably depicting clothing, skin texture, hair, etc.

- No visible noise or blur; extremely clear image.

- \*\*Score\*\*: 5

### Output Template (Please use only English output, and do not include parentheses in the output. Instead, fill in the parentheses directly according to the prompts in the template below.)

Static Clarity: (If there is visible blur, blockiness, jagged edges, or noise, please specify.) (Describe the specific content of the scene, focusing on the clothing and hair of the characters.) Are the details natural and realistic? Are the colors smooth?

Dynamic Clarity: Is there motion? (If so, indicate what kind of motion.) How is the clarity during motion? Are there any problems? (If so, please specify the problems.)

Overall Clarity: Overall clarity quality (enter evaluation keywords). (If the clarity score reaches 5, please add: the picture quality reaches 1080p or higher). Specifically describe the details and textures of the video content (if there is human hair, please include the hair's appearance).

Figure 6. Prompt used for rationale expansion on Clarity Quality.

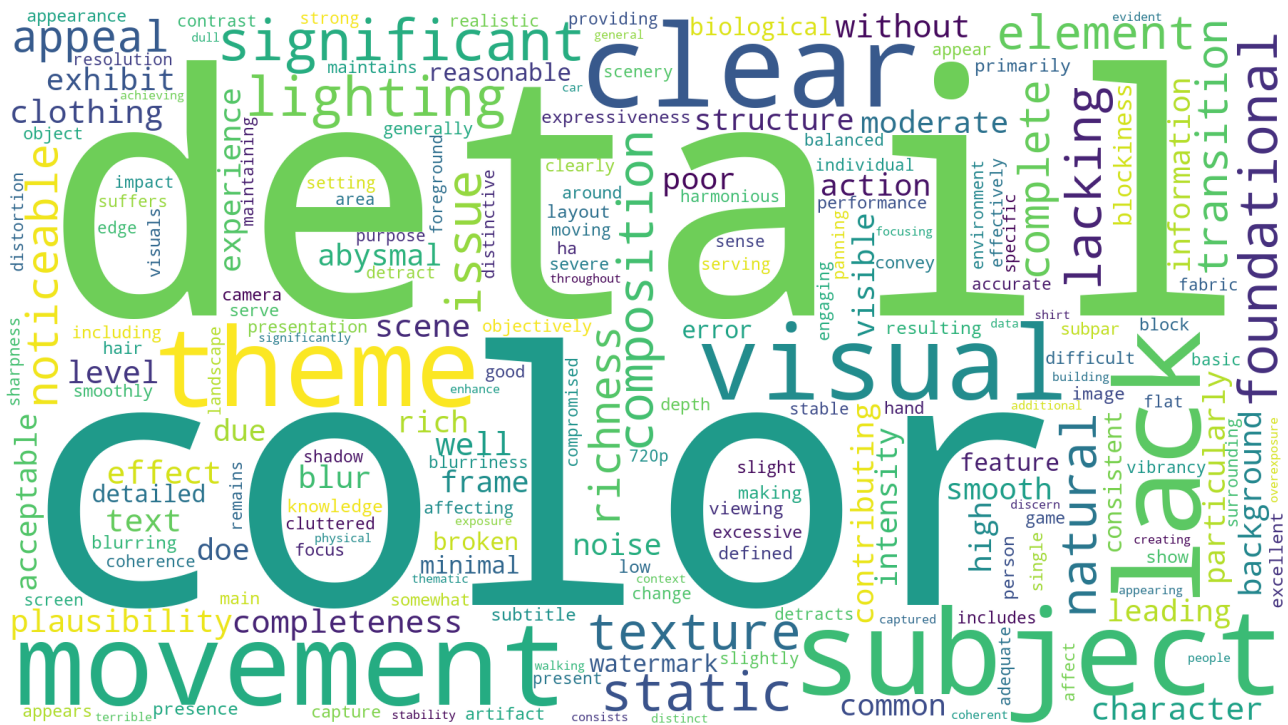


Figure 7. Word cloud display of rationale expansion.